The Design, Fabrication, and Application of Diamond Machined Null Lenses for Testing Generalized Aspheric Surfaces

James T. McCann

OFC - Diamond Turning Division
69T Island Street, Keene New Hampshire 03431

Abstract

This paper describes the optical design, fabrication and use of single element null lenses for the interferometric testing of generalized aspheric surfaces. The aspheric singlet is designed to work in collimated light, without a field lens, and allows for measurement of surface figure error over the entire clear aperture. The null lens is a single element of multispectral zinc sulfide (ZnS). This material is durable, easily diamond machined and provides good transmission at the test wavelength of 0.6328(4.. All reference surfaces needed for alignment are diamond machined into simple collars that hold the null lens and surface under test. This allows easy and accurate optical alignment and minimizes setup time.

The procedures for optical layout and alignment will be discussed as well as an error analysis including fabrication and alignment sensitivities. Several examples of the use of this element for testing aspheric surfaces will illustrate the technique. Finally, an extension of the technique to diffractive null optics will be presented.

Introduction

With the recent advances in the generation of aspheric surfaces, especially with diamond turning, there is a concomitant need to accurately and reliably test these surfaces. There have been many methods developed and applied to aspheric testing using both null optics,112'3 and contact profilometry4. Null tests using lenses and mirrors
have been employed from the earliest usage of aspherics and there are standard means for implementing some of these tests5. The applications presented in this paper use diamond turning to fabricate a single element null lens suitable for testing extremely fast asphercs. Although the layout of the optical test follows standard first order principles, the actual design of the lens makes use ofoptomechanics to ease fabrication, verification and alignment.
The generalized null lens test is shown in Figure 1.

The input light is a well-corrected axial point source, possibly at infinity, that normally is provided by an interferometer. The light is refracted by the null lens to form an aspheric wavefront whose caustic matches that of the surface under test near its center of curvature. Thus, the wavefront incident on the surface under test is retro-reflected through the null lens and returns to the source conjugate. In the absence of surface errors, all optical paths are equal and a null condition is obtained.

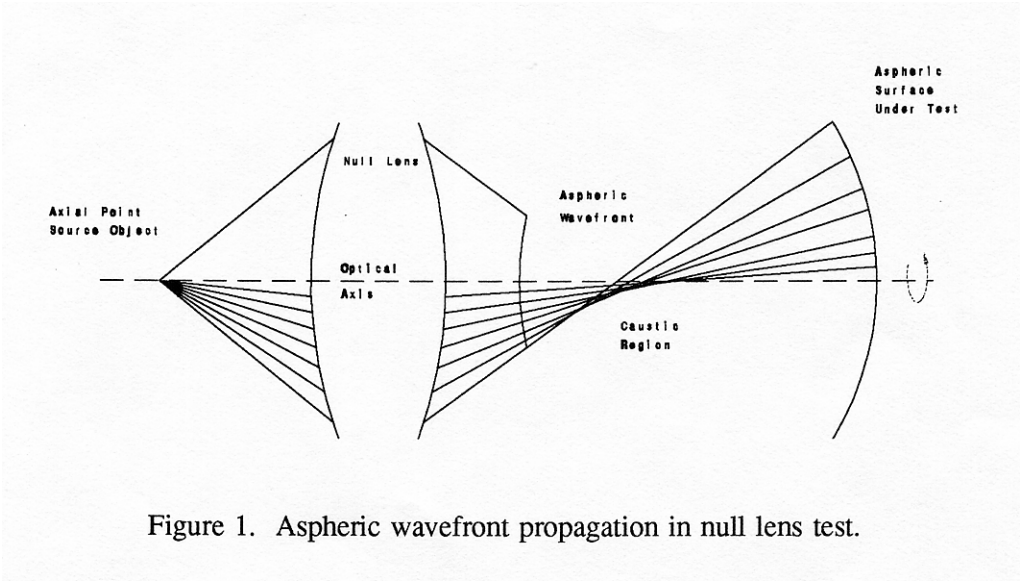

Figure 1. Aspheric wavefront propagation in null lens test.

Design Methodology

The general solution requires the placement of a centered aspheric surface somewhere in the optical path to null the wavefront from the surface under test6. If essentially all of the power and correction is on one surface of a lens, the other surface can be flat, and the lens fabrication is straightforward. With diamond turning this is possible.

^ Figure 2 illustrates the basic parameters of the null element. It has a plano-convex shape where the plane side is polished flat and the convex side is a generalized asphere. The element material has to satisfy three criteria. One, it has to be highly transmissive at 0.6328U.; two, it must be easily diamond machinable; and three, it must be durable so as to hold good figure accuracy after machining. Multispectral optical grade zinc sulfide (ZnS) is the material of choice here. Other materials do not satisfy all three criteria. Glass satisfies one and three, while acrylic satisfies one and two, so these materials cannot be used. Other diamond machinable materials such as zinc selenide (ZnSe) and calcium fluoride (CaF;) do not satisfy all three criteria as well as ZnS. In addition, the high index of refraction of ZnS allows shallow surfaces, making the fabrication (tool sweep errors) and verification (slope limitations) easier and more reliable.

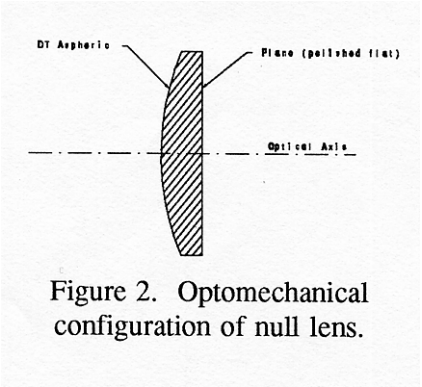

Figure 2. Optomechanical configuration of null lens.

The basic shape of the null lens is shown in Figure 2 and initially has the following parameters:

Clear aperture: 1 inch

Index of refraction at 632.8 nm: 2.35086

Center thickness: 0.250

^ Test Layout

The basic optical test layout is shown in Figure 3 from which the first order parameters will be derived.

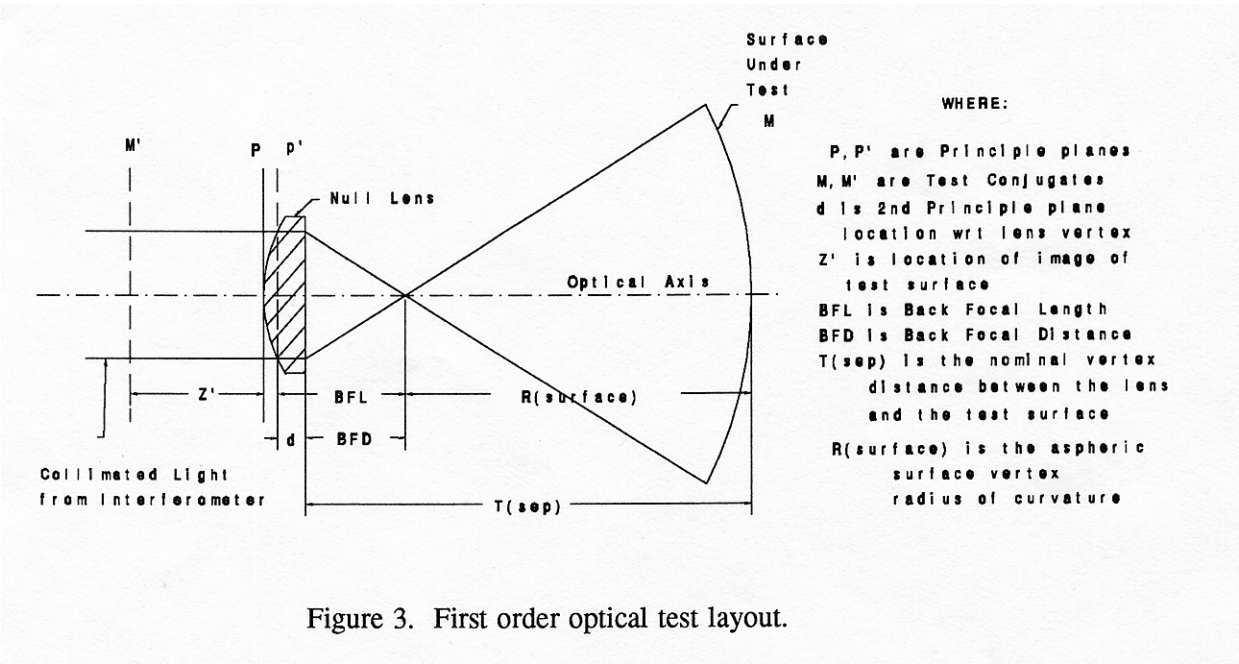

Figure 3. First order optical test layout.

"~ The first step is to calculate the focal length of the null lens. Since the input is collimated light from the interferometer, a good starting point is to match (to first order) the F/# of the lens to the R/# of the surface under test. If a suitable clear diameter for the lens is chosen, one inch for example, then the relationship is as follows:

$$(R/\#)_{surface} = (F/\#)_{lens} = (F_{lens})/(D_{lens}) = (F_{lens}/1'') = |F_{lens}|$$

$$Thus, \quad |F_{lens}| = (R/\#)_{surface}$$

Since the null lens is given a plano-convex shape, the radius of curvature of the 1st surface is easily calculated as follows:

$$\Phi_{lens} = \Phi_1 + \Phi_2 - \Phi_1\Phi_2\tau \quad , \textit{Lens power}$$

$$\Phi_1 = \frac{(N-1)}{R_1}; \; \Phi_2 = \frac{(1-N)}{R_2} = 0 \quad (since \; R_2 = \infty); \quad \tau = \frac{t_{lens}}{N}$$

$$Thus, \quad \Phi_{lens} = \Phi_1 = \frac{(N-1)}{R_1} \quad and \quad \underline{R_1 = (N-1)F_{lens}}$$

The initial vertex separation is given by the sum of the back focal distance and the mirror radius of curvature:

$$t_{sep} = BFD + R_{surface} = R_{surface} + BFL - \delta_{v'p'}$$

$$where, \quad \delta_{v'p'} = \frac{\Phi_1 t_{lens}}{\Phi_{lens} N}, \quad 2nd\ principle\ plane\ location$$

$$since, \quad \Phi_1 = \Phi_{lens}; \quad \delta_{v'p'} = \frac{t_{lens}}{N}$$

Thus, the initial parameters are:

$$t_{sep} = R_{surface} + F_{lens} - \frac{t_{lens}}{N}$$

$$with, \quad R_1 = (N-1)F_{lens}$$

The remaining task is to optimize the aspheric coefficients of surface 1 using a suitable lens design code and, if necessary, optimize the lens's radius of curvature and vertex separation to obtain a good solution. This will be illustrated in the following applications.

Application I - Infrared Lens Aspheric Surface Test

The first application is for testing a diamond machined aspheric surface on a germanium lens. This lens has a meniscus shape with a spherical surface on its convex side and a generalized asphere on its concave side. The optical test layout is shown in Figure 4.

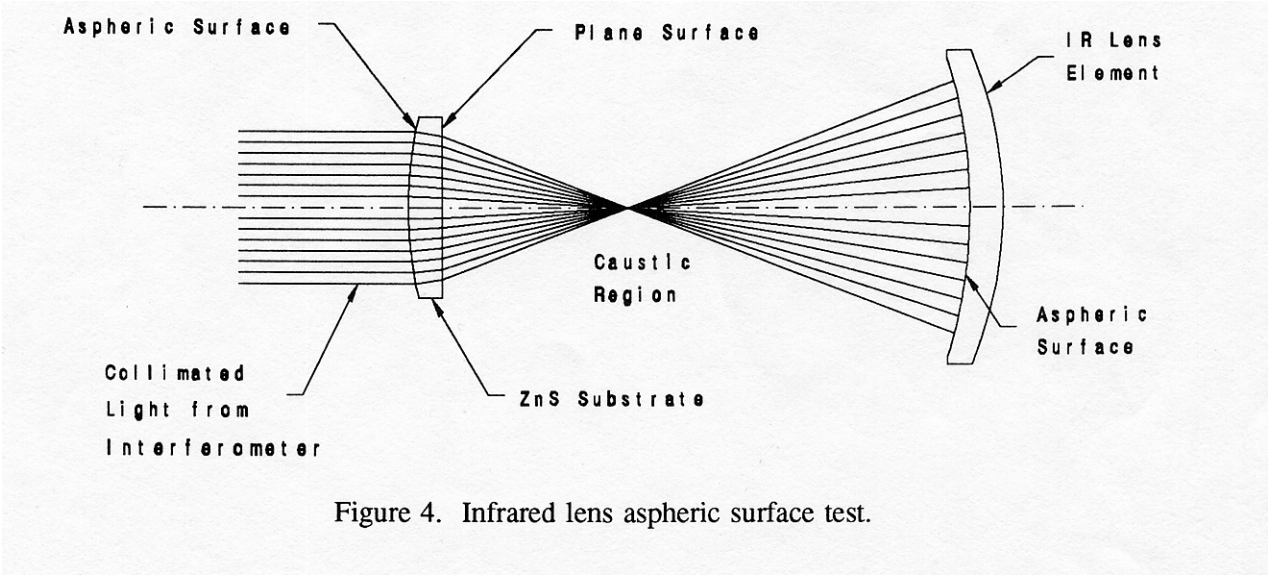

Figure 4. Infrared lens aspheric surface test.

^ The asphere is a modified conic section with additional aspheric terms to the 10th order. The parameters of this surface are as follows:

Clear aperture: 1.8 inches diameter
Vertex radius of curvature: 2.5505 inches
R/# of surface: 1.417
Surface figure requirement: ^ 4X PV @ 0.6328u,

Applying the first order principles of the last section, the null lens has a focal length of 1.417 inches (for a clear diameter of 1"). Since the refractive index of ZnS at 0.6328u, is 2.35086, the radius of curvature of the first surface is 1.914 inches. The location of the 2nd principle plane of the lens is -.1063" from the piano vertex and the initial vertex separation is 3.8612". Final optimization requires a change in radius of curvature to 1.98" and vertex spacing to 3.9 II". The residual OPD after optimization is ^0.01^,.

Figure 5 shows the optical test. The null lens is shown in front of the germanium lens. The first step in alignment is to square the null lens to the interferometer. Then the surface under test is aligned next. The flat ring on the outside of the surface is diamond machined perpendicular to the aspheric axis during the same setup as contouring and it is used for tipAilt. Final alignment of the pan is accomplished by translation in X,Y to eliminate tilt fringes and translation in Z (focus) to the proper axial spacing.

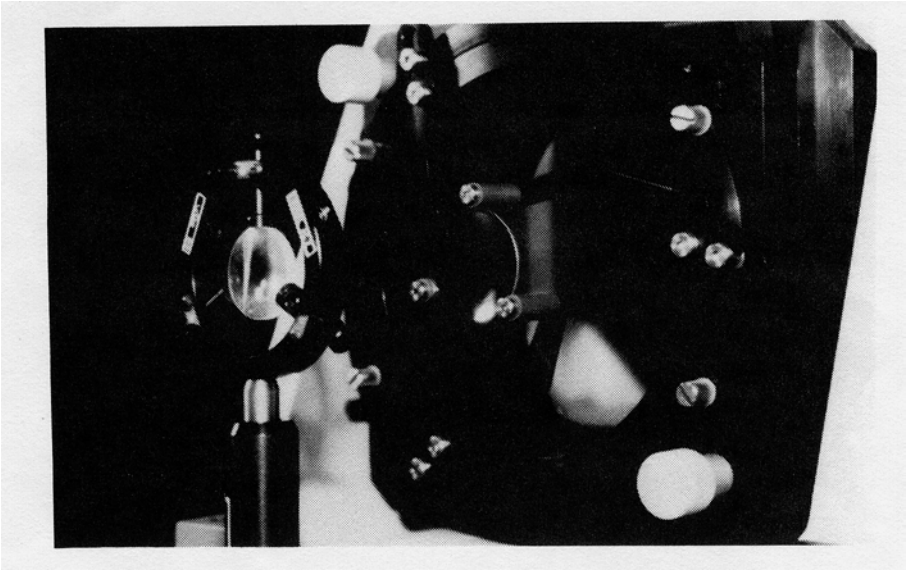

Figure 6 shows an interferogram of the aspheric surface with some tilt added. Figure 7 shows an OPD analysis of the surface errors. The surface error is l.OX PV which is much less than the requirement of ^4X PV.

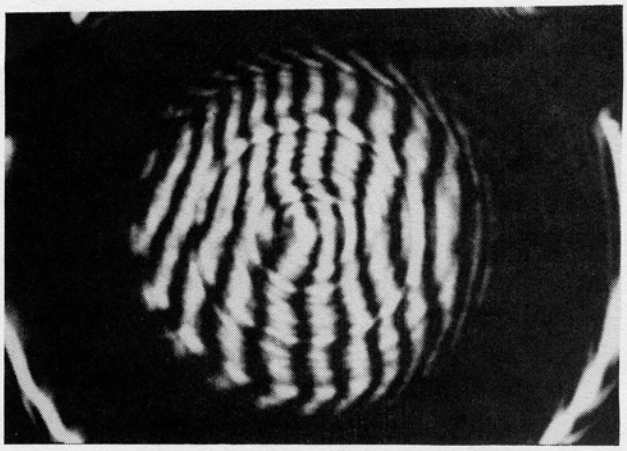

Figure 6. Single pass wavefront off lens surface.

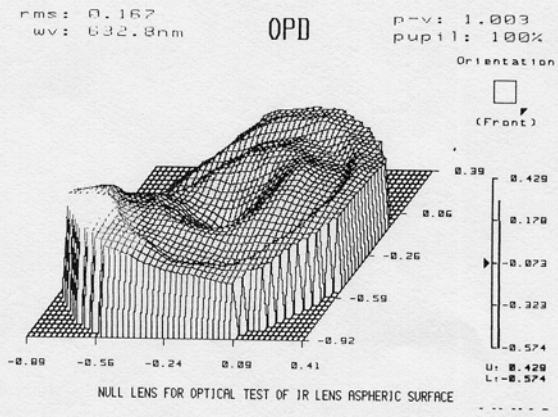

Figure 7. OPD analysis of interferogram.

Application II - On-Axis Aspheric Mirror with Racetrack Aperture

The second application of the technique is the null test of an aspheric mirror as shown in Figure 8. This mirror is the tertiary for a three mirror anastigmat (TMA) system. The system is designed to work in the visible and so the mirrors, including the tertiary, have tight surface specifications that require postpolishing. The null lens is used to guide the polisher through the final figuring and finishing.

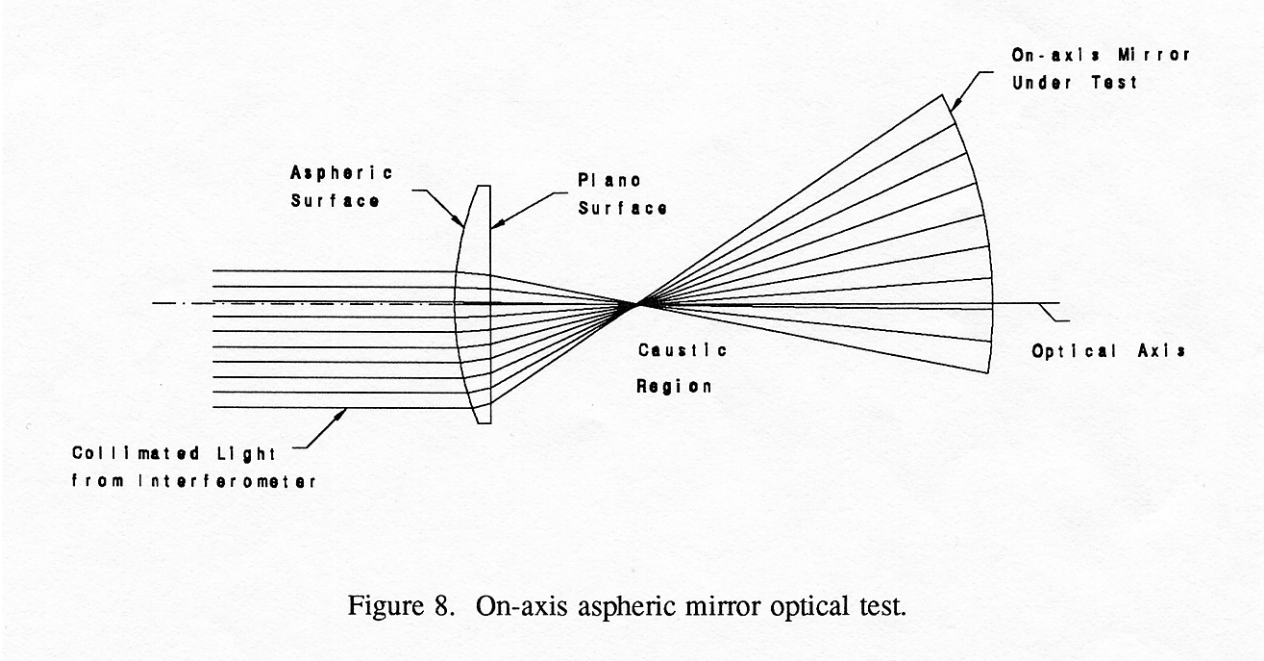

Figure 8. On-axis aspheric mirror optical test.

The mirror has a decentered racetrack aperture but has a physical center as shown in Figure 9.

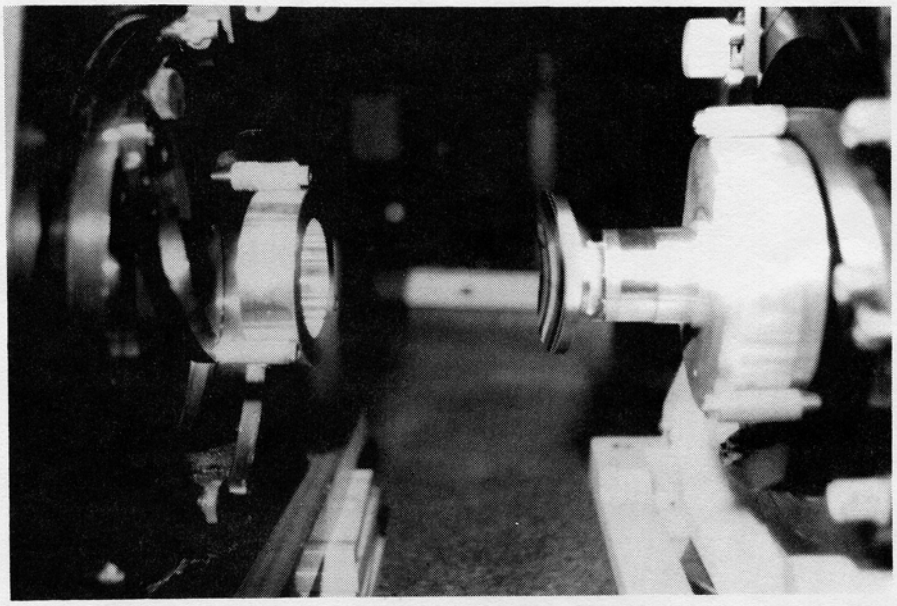

Figure 9. Optical test of on-axis aspheric mirror.

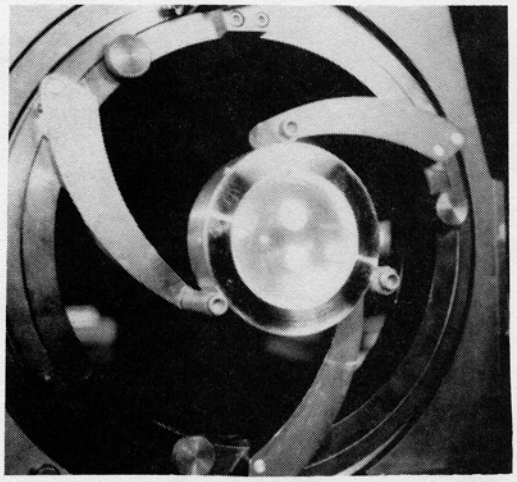

Figure 10. Null lens mounted in alignment collar.

In this application, a special collar was designed to hold the null lens as shown in Figure 10. This collar performed three important functions. One, it allowed for strong clamping on the edge without damaging the lens. Two, it has diamond machined mounting and reference surfaces that are parallel so as to allow easy alignment to the interferometer. Three, it provides a good structure for handling and storage of the lens.

The parameters of this surface are as follows:

Clear diameter:	3.1 inches
Vertex radius :	2.8982 inches
R/# of surface:	0.9349
Surface figure:	≤ 1λ PV at 0.6328μ

Applying the layout equations, the focal length is 0.9349 inches for the null lens. This gives a first surface radius of curvature of 1.2629 inches and an initial vertex separation of 4.0548 inches. Final optimization resulted in a radius of curvature of 1.86 inches and vertex separation of 4.148 inches. Final residual OPD is ^.OOlX,.

Figure 11 shows the single pass interferogram of the mirror during the initial postpolishing phase. Figure 12 shows an OPD analysis of the surface errors.

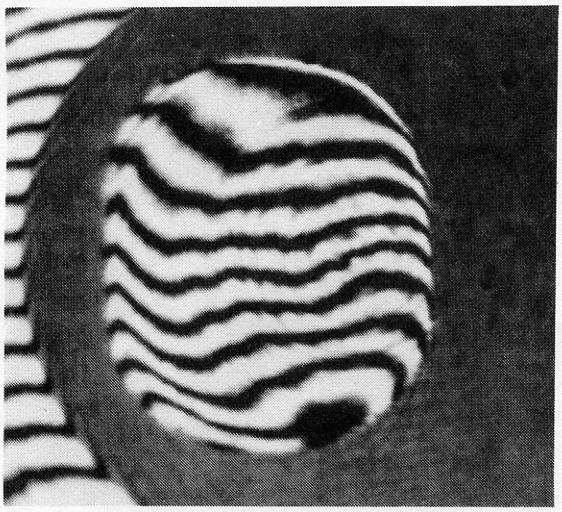

Figure 11. Single pass wavefront off aspheric mirror.

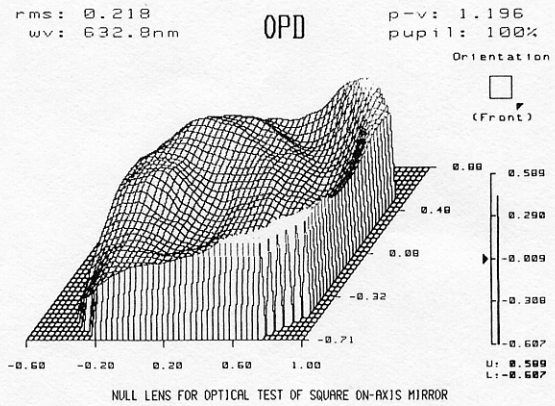

Figure 12. OPD analysis of interferogram.

Fabrication, Alignment and Test Considerations

Fabrication errors

This section will describe error contributions to the test wavefront due to null lens fabrication. These can come from four basic sources:

1) Diamond turned aspheric surface errors
2) Power & irregularity in the flat
3) Thickness variations
4) Index of refraction inhomogeneity

The surface error from the diamond turned asphere is radially symmetric and contributes a wavefront error in double pass of:

$$OPD_{PV}\ (waves) = \frac{2(N-1)\Delta H}{\lambda},\quad \textit{where } \Delta H \textit{ is the PV surface error;}$$

$$\lambda \textit{ is the wavelength, and } N \textit{ is the refractive index}$$

Irregularity in the polished flat surface usually takes the form of astigmatism and is bilaterally symmetric. If this parameter is specified in fringes, then:

$$OPD_{PV}\ (waves) = \frac{(N-1)(\#F)}{\lambda},\quad \textit{where } (\#F) \textit{ is the irregularity in fringes}$$

Index of refraction inhomogeneity contributes an error to the wavefront that is assumed to be randomly distributed. In double pass this wavefront error can be expressed as:

$$OPD_{PV}\ (waves) = \frac{2(\Delta N)T}{\lambda},\quad where$$

ΔN *is the index inhomogeneity, and* T *is the lens thickness*

The basic compensating parameter is the lens-to-surface vertex spacing. Surface power error and lens thickness error can essentially be eliminated by changing this parameter as shown in Table I.

Table I. Null lens compensating parameters.

Error	Amount	OPD_{PV} Increase	Despace Amount	Residual OPD_{PV}
Power	±1 Fringe	0.95	± 0.002"	0.03
Thickness	± 0.001"	0.17	± 0.0004"	0.005

In summary, typical error contributions are shown in Table II. This study uses the example from Application I.

Table II. Null lens fabrication induced wavefront errors.

Parameters	Error	OPD_{PV}	Comments
Aspheric	λ/8 PV	0.34	$N_{ZnS} \approx 2.351$
Flat	1/8 Fringe	0.17	Irregularity
Thickness	± 0.001"	0.005	Residual
Index	5 ppm	0.24	Typical
Σ_{RSS}	------→	0.45_{PV}	$\approx 0.11_{RMS}$

Alignment Sensitivities

This section will discuss wavefront errors that can occur in the alignment of the optical test. The accuracy in positioning is a critical factor in obtaining a reliable test result especially when aligning two relatively fast aspheres. The alignment sensitivity is determined by computing the change in both Peak-to-Valley and RMS wavefront error due to a small change in a particular alignment parameter. The alignment parameters studied are decenter, despace (defocus) and angular (tip/tilt). Since the test system is circularly symmetric (i.e. ±AX = ±AY etc.), misalignments in only one direction need to be analyzed. Table III shows the relevant alignment sensitivities of the null lens using the test layout of Application I.

Table III. Null lens optical test alignment sensitivities.

Alignment Parameter	Change in Parameter	Change in Wavefront Error	
		P-V	RMS
Decenter $\pm\Delta r$	±0.0005"	1.13	0.22
Despace $\pm\Delta z$	±0.001"	0.23	0.07
Angular $\pm\Delta\theta$	±100 μrad	0.10	0.02

It is clear from Table III that decenter is the most sensitive parameter. This is not surprising since the speed of the null lens is approximately F/1.5 and we must align two generalized aspheres. Most mechanical mounts allow for smooth motion of the optic and essentially infinite resolution in position. The key is to align the null lens accurately to the interferometer and then use the interference pattern to obtain final alignment of the surface under test. Since diamond machining errors on rotationally symmetric surfaces tend also to be rotationally symmetric, any asymmetry in the wavefront such as coma, is likely to be caused by misalignments.

Visibility Estimate

Visibility of the fringe pattern is found to be adequate without any antireflection coating on the lens surfaces. The following analysis will estimate the fringe visibility using two beam interference'. Several assumptions will be made in the analysis. One, that the Fresnel equations for normal incidence can be used; two, that there is no absorption; and three, that reasonable estimates for the reflectivity of the surface under test can be made. In Figure 13, the test parameters used in the analysis are shown.

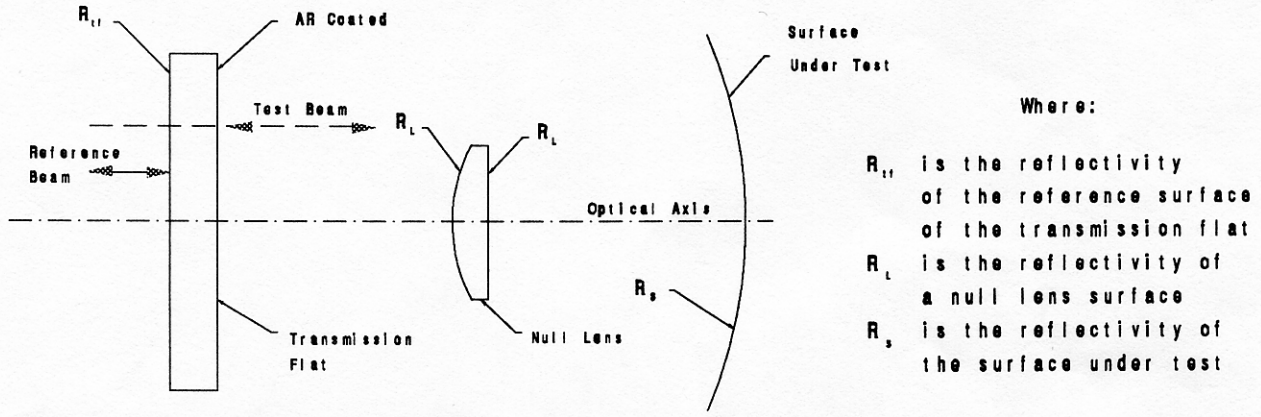

Figure 13. Layout for visibility analysis.

The test and reference beam intensities, I_T and I_R, can be defined according to the above as follows:

$$I_R = I_0 R_{tf} \quad \textit{and} \quad I_T = I_0(1-R_{tf})^2(1-R_L)^4 R_S$$

The visibility is given by the following relations:

$$V = \frac{(I_{max}-I_{min})}{(I_{max}+I_{min})} \quad where,$$

$$I_{max} = I_T+I_R+2(I_TI_R)^{1/2} \quad and \quad I_{min} = I_T+I_R-2(I_TI_R)^{1/2}$$

$$Thus, \quad V = \frac{2(I_TI_R)^{1/2}}{(I_T+I_R)}$$

In our test setup reasonable values for the reflectivities are obtained as follows:

$$R_L \sim [\frac{(N-1)}{(N+1)}]^2 = 0.16, \text{ for } N \sim 2.35$$

$$R_{ff} \sim 0.04, \text{ Fresnel reflection}$$

$$R_S \sim 0.90, (< \text{for lens}, > \text{for mirror})$$

$$Thus, \ I_R = (.04)I_0 \text{ and } I_T = (1-.04)^2(1-.16)^4(.90) = 0.413I_0$$

$$and, \quad V = 0.57$$

If a pellicle is added to the test path (R=0.75), then:

IT - 0.413/o(.25)2 and, V - 0.98

Future Directions

Since diamond turning can generate any rotationally symmetric surface, it seems a natural and logical extension to apply diffractive phase structures to the null lens solution. To illustrate the technique, a diffractive phase structure was designed on a multispectral ZnS substrate to replace the null lens in Application I. The optical test layout is shown in Figure 14.

The substrate is a plano-plano window that is 1 inch in diameter and l/h inch thick. The diffractive phase profile is on the side facing the surface under test. The equation describing the phase profile is rotationally symmetric and is of the form:

$$\Phi(r) = \frac{2\pi}{\lambda_0}[Ar^2+Br^4+Cr^6+....]$$

where r is the radial coordinate of the phase profile and A,B,C, etc. are the aberration correction coefficients which are determined during optimization.

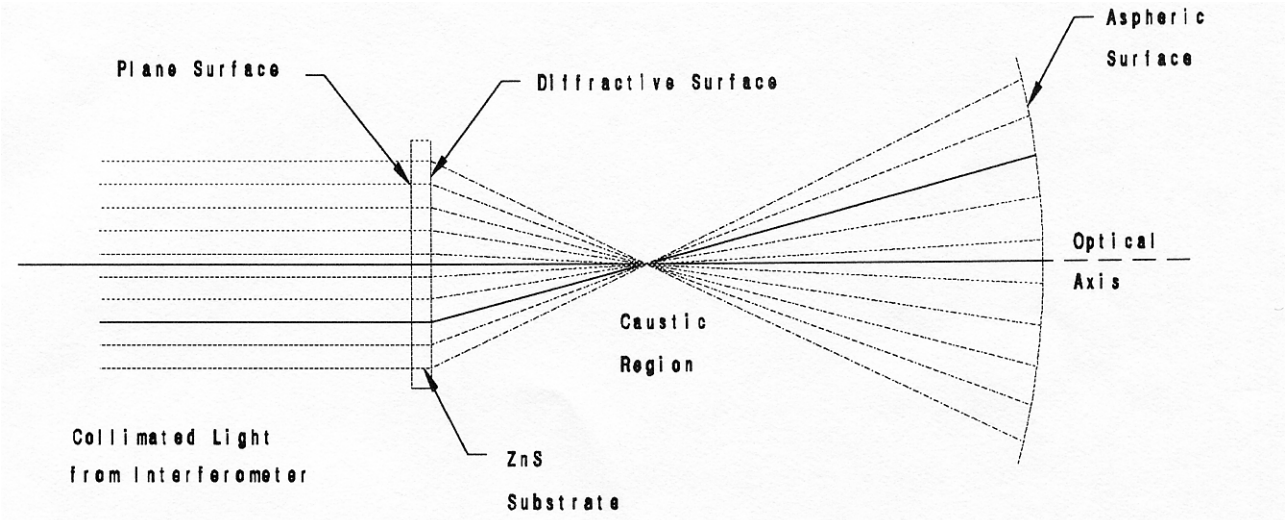

Figure 14. Diffractive null optical test layout.

An adequate solution is obtained by using phase coefficients to the 12th order. Figures 15 and 16 show the diffractive lens and the residual OPD error respectively.

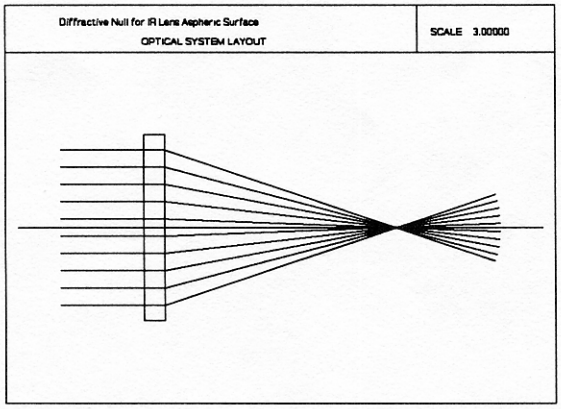

Figure 15. Diffractive null lens.

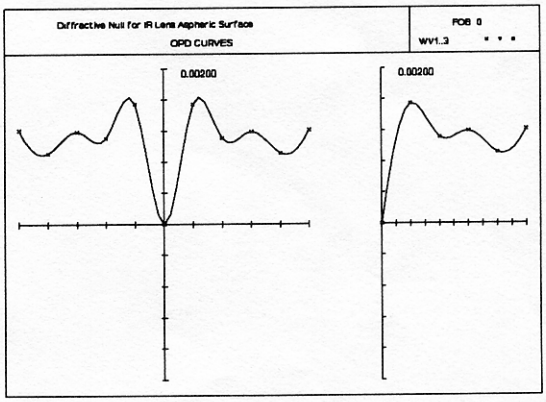

Figure 16. Residual OPD of null optic.

The advantages of this approach are many. First, the blank is cheaper and easier to get. It can be stocked in-house for rapid turnaround which is a big advantage in a production environment where quick design and fabrication of null optics is necessary for timely delivery of parts. Another advantage is alignment ease. One need only collimate off the flat first surface to square the null optic to the beam. Since all the power and aberration correction is on the second surface there is no restriction on thickness. This also means that no centering relationship of the diffractive surface to the first surface needs to be maintained as there is for a lens. Refractive index inhomogeneity is still a problem, but the substrate can be much thinner than the lens, thus reducing this effect.

In summary, the use of a single diffractive phase profile on a simple substrate can reduce the fabrication errors to that of a single surface, as one would have for a null reflector. The application of diamond turning to fabricate these structures has been demonstrated8 and proven to be viable method. This promises to be a technique that has tremendous advantages in future aspheric testing.

Conclusions

The use of diamond turning to fabricate null lenses has been shown to be a great advantage for optical fabrication and testing. By designing the lens to be plano-convex and putting all the required aspheric correction on one surface, a lens is obtained that is mechanically simple, easy to machine and qualify, and quick to align. No other lenses such as field lenses are required, and this technique allows testing of very fast aspherics. The further application of diffractive optics promises to extend the tools of general aspheric metrology.

References

^M.C. Gerchman, "Testing generalized rotationally-symmetric aspheric optical surfaces using null reflective compensating components", SPIE Proc., Vol. 676, pp. 59-65 (1987).

^.T. McCann, "Applications of diamond turned null reflectors for generalized aspheric metrology", SPIE Proc., Vol. 1332,(1990).

M.G. Stevens and R.K.Morton, "A unique solution to aspheric measurement and analysis as part of a manufacturing process", SPIE Proc., Vol. 966, pp. 150-156, (1988).

^.T. Holleran, "An algebraic solution for the small lens null compensator", Applied Optics, Vol. 7, January 1968, Pg. 137.

^ Offher, "Null tests using compensators", Optical Shoo Testins, D. Malacara, Chap. 14, pp.439-458, John Wiley and Sons, (1978).

'M Born and E. Wolf, Principles of Optics, Chapter 4, pg. 197, Pergamon Press, (1975)

"M.C. Gerchman and G.C. Hunter, "Differential technique for accurately measuring the radius of curvature of long radius concave optical surfaces", SPIE Proc., Vol. 192, pp. 80-82, (1979).

"MJ. Riedl and J.T. McCann, "Analysis and performance limits of diamond turned diffractive lenses for the 3-5 and 8-12 micrometer regions", SPIE Proc., Vol. CR 38, (1991).